

# Probe of extra dimensions in $\gamma q \rightarrow \gamma q$ at the LHC

İ. Şahin,<sup>1,\*</sup> A. A. Billur,<sup>2,†</sup> S. C. İnan,<sup>2,‡</sup> B. Şahin,<sup>1,§</sup>

M. Köksal,<sup>2,¶</sup> P. Tektaş,<sup>3</sup> E. Alıcı,<sup>3</sup> and R. Yıldırım<sup>2</sup>

<sup>1</sup>*Department of Physics, Faculty of Sciences,*

*Ankara University, 06100 Tandogan, Ankara, Turkey*

<sup>2</sup>*Department of Physics, Cumhuriyet University, 58140 Sivas, Turkey*

<sup>3</sup>*Department of Physics, Bulent Ecevit University, 67100 Zonguldak, Turkey*

## Abstract

We have examined TeV scale effects of extra spatial dimensions through the processes  $\gamma q \rightarrow \gamma q$  where  $q = u, d, c, s, b, \bar{u}, \bar{d}, \bar{c}, \bar{s}, \bar{b}$ . These processes have been treated in a photon-proton collision via the main reaction  $pp \rightarrow p\gamma p \rightarrow p\gamma qX$  at the LHC. We have employed equivalent photon approximation for incoming photon beams and performed statistical analysis for various forward detector acceptances.

---

\*inancsahin@ankara.edu.tr

†abillur@cumhuriyet.edu.tr

‡sceminan@cumhuriyet.edu.tr

§banusahin@ankara.edu.tr

¶mkoksal@cumhuriyet.edu.tr

## I. INTRODUCTION

Extra spatial dimensions that show themselves near the TeV scale have been widely studied in particle physics since the pioneering works of Arkani-Hamed, Dimopoulos and Dvali (ADD) [1–3]. Soon after the work of ADD a warped model was proposed by Randall and Sundrum (RS) [4]. According to ADD and RS models, extra spatial dimensions can have observable effects at the TeV scale physics. The possibility of these extra dimensions has been probed in the past colliders but no evidence has been found. The Large Hadron Collider (LHC) offers the opportunity of a very rich physics program. Signals confirming the existence of extra dimensions might become detectable in the high energetic collisions of the LHC. Phenomenological studies on extra dimensions involving quark-quark, gluon-gluon or quark-gluon collisions at the LHC are widespread in the literature. On the other hand, extra dimensions have been much less studied in photon-induced reactions ( $\gamma\gamma$  or  $\gamma$ -proton collisions) at the LHC.

In an usual proton-proton deep inelastic scattering (DIS) processes both of the incoming protons dissociate into partons. Due to proton remnants, usual DIS processes do not provide a clean environment. Jets coming from proton remnants create some uncertainties and make it difficult to discern the signals which may arise from the new physics beyond the standard model. On the other hand, in  $\gamma\gamma$  or  $\gamma$ -proton collisions with quasireal photons, photon emitting protons remains intact.  $\gamma\gamma$  processes provide the most clean channels due to absence of the remnants of both proton beams. Whereas in  $\gamma$ -proton processes one of the incoming protons dissociates into partons but other proton remains intact. Midway from proton-proton DIS to  $\gamma\gamma$ ,  $\gamma$ -proton processes have less experimental uncertainties compared with proton-proton processes. Furthermore, they have higher energy reach and effective luminosity with respect to  $\gamma\gamma$  processes [5–7].

In this work we have investigated TeV scale effects of extra spatial dimensions via the process  $\gamma q \rightarrow \gamma q$  at the LHC. The process  $\gamma q \rightarrow \gamma q$  takes part as a subprocess in the main reaction  $pp \rightarrow p\gamma p \rightarrow p\gamma q X$  (Fig.1). The photon which enters the subprocess is emitted from one of the proton beams and described by equivalent photon approximation (EPA) [8–10]. In the framework of EPA, virtuality of the quasireal photons is very low. Hence when a proton emits a quasireal photon, it does not dissociate into partons. In EPA, quasireal photons carry a small transverse momentum. Therefore photon emitting intact protons

deviate slightly from their trajectory along the beam path. They are generally scattered with very small angles from the beam pipe and exit the central detector without being detected. Consequently, detection of intact protons needs forward detector equipment in addition to central detectors. It is foreseen to equip ATLAS and CMS central detectors with very forward detectors which can detect intact scattered protons with a very large pseudorapidity. A project called AFP (ATLAS Forward Physics) that aims to install very forward detectors located at distances 220 and 420 m from the interaction point, is under evaluation in the ATLAS collaboration [11, 12]. The acceptance proposed by AFP project is  $0.0015 < \xi < 0.15$  where  $\xi$  is the momentum fraction loss of the intact scattered protons. Mathematically speaking, it is defined by the formula  $\xi = (|\vec{p}| - |\vec{p}'|)/|\vec{p}|$ . Here  $\vec{p}$  is the momentum of incoming proton and  $\vec{p}'$  is the momentum of intact scattered proton. At the LHC energies, it is a good approximation to write  $\xi = \frac{E_\gamma}{E}$  where  $E_\gamma$  is the energy of the emitted quasireal photon and  $E$  is the energy of the incoming proton. There are also other scenarios with different acceptances. When forward detectors are placed closer to the interaction point they can detect protons with higher  $\xi$ . In the CMS-TOTEM forward detector scenario, a forward detector acceptance of  $0.0015 < \xi < 0.5$  is considered [13, 14]. This wide acceptance range is provided by the use of the detectors of TOTEM experiment at 147 and 220 m from the CMS interaction point in addition to forward detectors at 420 m.

Existence of photon-induced reactions in a hadron collider is not merely a theoretical hypothesis. Photon-induced reactions in a hadron-hadron collision were verified experimentally at the Fermilab Tevatron [15–17]. The reactions such as  $p\bar{p} \rightarrow p\gamma\gamma\bar{p} \rightarrow pe^+e^-\bar{p}$  [15, 16],  $p\bar{p} \rightarrow p\gamma\gamma\bar{p} \rightarrow p\mu^+\mu^-\bar{p}$  [16, 17],  $p\bar{p} \rightarrow p\gamma\bar{p} \rightarrow pJ/\psi(\psi(2S))\bar{p}$  [17] were observed by the CDF collaboration. From the early LHC data obtained in proton-proton collisions at  $\sqrt{s} = 7$  TeV, two-photon reactions  $pp \rightarrow p\gamma\gamma p \rightarrow p\mu^+\mu^-p$  and  $pp \rightarrow p\gamma\gamma p \rightarrow pe^+e^-p$  have been observed by the CMS Collaboration [18, 19]. Probing new physics via photon-photon and photon-proton reactions at the LHC has been studied in the literature. Phenomenological studies cover a wide range of new physics such as supersymmetry, extra dimensions, unparticle physics, anomalous interaction of standard model particles, magnetic monopoles, etc. [6, 14, 20–46].

In this paper we aim to constrain model parameters of ADD and RS models in a *quasireal photon-proton* deep inelastic scattering process. As far as we know, ADD or RS model of ex-

tra dimensions has not been studied and model parameters have not been constrained in any phenomenological study in the context of *quasireal photon-proton* deep inelastic scattering at the LHC. The subprocess  $\gamma q \rightarrow \gamma q$  that we have considered, is the simplest process which appears in a photon-proton collision. It is very similar to Compton scattering which is one of the fundamental processes in particle physics.  $\gamma q \rightarrow \gamma q$  may take part as a subprocess in any reaction where the electromagnetic interaction of quarks is considered. Hence, it is important to know the effect of new physics coming from extra dimensional theories to this particular process.

## II. ADD MODEL OF LARGE EXTRA DIMENSIONS

ADD model was proposed as a solution to the hierarchy problem which is known as the unexplained large difference between the electroweak scale  $\sim \mathcal{O}(100 \text{ GeV})$  and the Planck scale  $M_{Pl} \sim \mathcal{O}(10^{19} \text{ GeV})$  [1–3]. According to ADD model, gravity can propagate in a  $4 + \delta$  dimensional space called "bulk" but Standard Model (SM) particles are confined in a hypersurface called "brane". Using Gauss' law in arbitrary dimensions, 4-dimensional Planck scale can be related to the  $(4 + \delta)$ -dimensional fundamental scale  $M_D$  through the formula

$$M_{Pl}^2 = 8\pi R^\delta M_D^{2+\delta}. \quad (1)$$

Here,  $R$  is the radius of the compactified extra dimensional space of dimension  $\delta$  and volume  $V_\delta = (2\pi R)^\delta$ . In the ADD model, the hierarchy is eliminated by choosing the compactification radius large. For instance if we choose  $R \sim 0.1 \text{ mm}$  for  $\delta = 2$  then  $M_D$  is at the order of  $\mathcal{O}(1 \text{ TeV})$ . An important consequence of large extra dimensions is the tower of Kaluza-Klein (KK) modes. Solutions of linear Einstein equations in  $4 + \delta$  dimension manifest themselves as a set of states separated in mass by  $\mathcal{O}(\frac{1}{R})$  in 4 dimension [47, 48]. In 4-dimensional effective theory we have spin-2 and spin-0 KK states that can interact with SM fields on the brane. Spin-2 and spin-0 states are sometimes called KK-gravitons and gravitational scalars respectively. KK-gravitons couple to the energy-momentum tensor of the SM fields. Although their coupling to SM fields is suppressed by a factor proportional to  $\frac{1}{M_{Pl}}$ , summation of enormous number of KK states in a tower provides an effective coupling of order  $\frac{1}{M_D}$ . Therefore, KK-gravitons can have observable effects at the TeV scale. Gravita-

tional scalars are coupled only to the trace of the energy-momentum tensor. Since the trace of the energy-momentum tensor is zero for massless particles, the coupling of gravitational scalar to photons is zero at the tree-level. Hence, we will neglect gravitational scalars during amplitude calculations. Feynman rules for KK-gravitons were given in [47, 48].

The process  $\gamma q \rightarrow \gamma q$  is described by 3 tree-level diagrams (Fig.2). The polarization summed amplitude square can be written as

$$|M|^2 = |M_{SM}|^2 + |M_{KK}|^2 + |M_{int}|^2 \quad (2)$$

where  $M_{SM}$  is the SM amplitude,  $M_{KK}$  is the amplitude for the t-channel KK-graviton exchange and  $|M_{int}|^2$  represents interference terms between the SM and the KK amplitudes. Analytical expressions for SM, KK and interference terms as a function of Mandelstam parameters  $\hat{s}$ ,  $\hat{t}$  and  $\hat{u}$  are

$$\begin{aligned} |M_{SM}|^2 = -8g_e^4 q^4 & \left[ \frac{1}{(\hat{s} - m_q^2)^2} [3m_q^4 + \hat{s}\hat{u} - m_q^2(5\hat{s} + 2\hat{t} + 3\hat{u})] \right. \\ & + \frac{1}{(\hat{u} - m_q^2)^2} [3m_q^4 + \hat{s}\hat{u} - m_q^2(3\hat{s} + 2\hat{t} + 5\hat{u})] \\ & \left. - \frac{2}{(\hat{s} - m_q^2)(\hat{u} - m_q^2)} [6m_q^4 + 2m_q^2\hat{t} - m_q^2(\hat{s} + 4\hat{t} + \hat{u})] \right] \quad (3) \end{aligned}$$

$$|M_{KK}|^2 = \frac{1}{2\bar{M}_{Pl}^4} |D(\hat{t})|^2 [(4m_q^2 - \hat{t})\hat{t} + (\hat{s} - \hat{u})^2] [2m_q^4 + \hat{s}^2 + \hat{u}^2 - 2m_q^2(\hat{s} - \hat{t} + \hat{u})] \quad (4)$$

$$\begin{aligned} |M_{int}|^2 = \frac{g_e^2 q^2 (D(\hat{t}) + D^*(\hat{t}))}{2\bar{M}_{Pl}^2} & \left\{ \frac{1}{(\hat{s} - m_q^2)} [8m_q^6 - 2m_q^4(\hat{s} - 5\hat{t} + 7\hat{u}) \right. \\ & + (\hat{s} - \hat{t} - \hat{u})(3\hat{s}^2 + 2\hat{s}\hat{t} + \hat{t}^2 - (\hat{s} + \hat{t})\hat{u}) \\ & + m_q^2(-3\hat{s}^2 + 10\hat{s}\hat{t} + \hat{t}^2 + 6\hat{s}\hat{u} - 2\hat{t}\hat{u} + 5\hat{u}^2)] \\ & \left. + (\hat{s} \longleftrightarrow \hat{u}) \right\} \quad (5) \end{aligned}$$

where  $g_e = \sqrt{4\pi\alpha}$  and  $m_q$  is the mass of the quark.  $q$  is the quark charge which is given in units of positron charge. In eqs.(3-5) we do not write the factor due to initial spin average.  $\bar{M}_{Pl} = M_{Pl}/\sqrt{8\pi}$  is the reduced Planck mass.  $D(\hat{t})$  denotes propagator factors which are summed over infinite tower of KK modes. The existence of this infinite sum

creates ultraviolet divergences even in tree-level processes. We employ the cutoff procedure that was assumed in Ref.[47] for phenomenological applications:

$$\frac{1}{\bar{M}_{Pl}^2} D(\hat{t}) = \frac{1}{\bar{M}_{Pl}^2} \sum_n \frac{1}{t - m_n^2} \equiv \frac{4\pi}{\Lambda_T^4} \quad \text{for } \delta > 2 \quad (6)$$

Here,  $\Lambda_T$  is an effective cutoff scale. Its dependence on  $M_D$  can be identified with some knowledge of the underlying quantum gravity theory. In case of string theory, the inequality  $M_D > \Lambda_T$  can be written [47]. As a consequence, any lower bound for  $\Lambda_T$  also serves as a lower bound for  $M_D$ .

The cross section for the main process  $pp \rightarrow p\gamma p \rightarrow p\gamma qX$  can be obtained by integrating the cross section for the subprocess  $\gamma q \rightarrow \gamma q$  over the photon and quark distributions:

$$\sigma(pp \rightarrow p\gamma p \rightarrow p\gamma qX) = \sum_q \int_{\xi_{min}}^{\xi_{max}} dx_1 \int_0^1 dx_2 \left( \frac{dN_\gamma}{dx_1} \right) \left( \frac{dN_q}{dx_2} \right) \hat{\sigma}_{\gamma q \rightarrow \gamma q}(\hat{s}) \quad (7)$$

where  $x_1$  is the fraction which represents the ratio between the scattered equivalent photon and initial proton energy and  $x_2$  is the momentum fraction of the proton's momentum carried by the struck quark.  $\frac{dN_\gamma}{dx_1}$  and  $\frac{dN_q}{dx_2}$  are the equivalent photon and quark distribution functions. Analytical expression for  $\frac{dN_\gamma}{dx_1}$  is given in the Appendix. Quark distribution functions have been evaluated numerically by using a code MSTW2008 [49]. The summation in (7) is performed over the following subprocesses:

$$\begin{aligned} \text{(i)} \quad & \gamma u \rightarrow \gamma u & \text{(vi)} \quad & \gamma \bar{u} \rightarrow \gamma \bar{u} \\ \text{(ii)} \quad & \gamma d \rightarrow \gamma d & \text{(vii)} \quad & \gamma \bar{d} \rightarrow \gamma \bar{d} \\ \text{(iii)} \quad & \gamma c \rightarrow \gamma c & \text{(viii)} \quad & \gamma \bar{c} \rightarrow \gamma \bar{c} \\ \text{(iv)} \quad & \gamma s \rightarrow \gamma s & \text{(ix)} \quad & \gamma \bar{s} \rightarrow \gamma \bar{s} \\ \text{(v)} \quad & \gamma b \rightarrow \gamma b & \text{(x)} \quad & \gamma \bar{b} \rightarrow \gamma \bar{b} \end{aligned} \quad (8)$$

During all calculations in this paper we assume that center-of-mass energy of the proton-proton system is 14 TeV.

We estimate the sensitivity of the reaction  $pp \rightarrow p\gamma p \rightarrow p\gamma qX$  to extra dimensions using a simple one parameter  $\chi^2$  criterion without a systematic error. The  $\chi^2$  function is given by

$$\chi^2 = \left( \frac{\sigma - \sigma_{SM}}{\sigma_{SM} \delta} \right)^2 \quad (9)$$

where  $\sigma$  is the cross section containing both SM and KK contributions,  $\sigma_{SM}$  is the SM cross section and  $\delta = \frac{1}{\sqrt{N}}$  is the statistical error. Cross sections used in the  $\chi^2$  function

are integrated total cross sections which are defined by Eq. (7). Hence, contributions from all subprocesses in (8) have been taken into account. During statistical analysis, the expected number of events is calculated through the formula:  $N = S \times E \times \sigma_{SM} \times L_{int}$ , where,  $L_{int}$  is the integrated luminosity,  $E$  is the jet reconstruction efficiency and  $S$  is the survival probability factor. We consider a survival probability factor of  $S = 0.7$  and jet reconstruction efficiency of  $E = 0.6$ . We have also imposed a pseudorapidity cut of  $|\eta| < 2.5$  for final (anti-)quarks and photons from subprocesses in (8). We have obtained 95% confidence level (C.L.) lower bounds for  $\Lambda_T$  considering forward detector acceptances of  $0.0015 < \xi < 0.15$ ,  $0.0015 < \xi < 0.5$ ,  $0.1 < \xi < 0.15$  and  $0.1 < \xi < 0.5$ . The first two are the AFP and CMS-TOTEM acceptances as we have mentioned in the introduction. The last two are the subintervals of the whole AFP and CMS-TOTEM acceptance regions. Forward detectors have a capability to detect intact protons in a continuous range of momentum fraction loss  $\xi$ . Hence, we can impose cuts and choose to work in a subinterval of the whole acceptance region. Since the KK terms in the amplitude square have a higher momentum dependence than the SM terms, imposing such cuts and removing low energy region of the whole acceptance range considerably suppress the SM contribution without minimizing the KK effects.

In Fig.3 we present 95% C.L. lower bounds for  $\Lambda_T$  as a function of integrated LHC luminosity for AFP and CMS-TOTEM acceptances. At the LHC energies, deep inelastic scattering processes generally have a very high virtuality. Due to Bjorken scaling it is expected that quark distribution functions do not depend significantly on  $Q^2$  but only on  $x$ . Hence, during numerical calculations a fix  $Q^2$  value can be used. Bjorken scaling is, however, not exact. For this reason, the bounds have been obtained by considering three different virtualities  $Q^2 = M_Z^2, (5M_Z)^2$  and  $(10M_Z)^2$  for the deep inelastic scattering where  $M_Z$  is the mass of the Z boson. Here,  $M_Z$  represents only a scale which is roughly at the order of Standard Model energies.  $Q = M_Z, 5M_Z$  and  $10M_Z$  are plausible scales for our process. For instance, if the center-of-mass energy of the subprocess  $\gamma q \rightarrow \gamma q$  is  $\sqrt{\hat{s}} = 180$  GeV and outgoing photon is scattered with an angle of 60 degree at the center-of-mass system of the incoming photon and quark then the square of the momentum transferred to the proton is  $q^2 = -(90\text{GeV})^2$ . Similarly for  $\sqrt{\hat{s}} = 900$  GeV and  $\sqrt{\hat{s}} = 1800$  GeV, the corresponding momentum squares are  $q^2 = -(450\text{GeV})^2$  and  $q^2 = -(900\text{GeV})^2$  respectively. In the laboratory system, incoming photon and quark do not have fix energies. Instead,

their energies are described by photon and quark distributions. If we assume that center-of-mass energy of the proton-proton system is  $\sqrt{s} = 14$  TeV and upper bound for the forward detector acceptance is 0.5 (0.15) then the center-of-mass energy of the subprocess extends up to energies of approximately 9900 GeV (5422 GeV). Hence, it is probable for our subprocess to possess a virtuality of  $Q^2 = M_Z^2, (5M_Z)^2$  or  $(10M_Z)^2$ .

In Fig.4 we present the lower bounds for  $0.1 < \xi < 0.15$  and  $0.1 < \xi < 0.5$  subintervals of the whole AFP and CMS-TOTEM acceptances. We see from these figures that the bounds for  $0.1 < \xi < 0.15$  and  $0.1 < \xi < 0.5$  cases are approximately 2 times stronger than the bounds for  $0.0015 < \xi < 0.15$  and  $0.0015 < \xi < 0.5$  respectively. We have exhibited in Fig.3 and Fig.4 that limits vary a little with  $Q^2$ . But the variation in limits is minor. To be precise, we see from the left panel of Fig.3 that limits vary approximately by a factor of 1.06 when the square root of the virtuality  $Q$  varies by a factor of 10. (or equivalently, virtuality  $Q^2$  varies by a factor of 100.)

### III. RS MODEL OF WARPED EXTRA DIMENSIONS

Although the ADD model eliminates the hierarchy between the electroweak scale and the Planck scale, it introduces a new hierarchy between the electroweak scale and  $\frac{1}{R}$ . In this respect, RS model solves the hierarchy problem without generating another large hierarchy. In the simplest RS model, we have only one extra spatial dimension and two branes located at orbifold fixed points  $y = 0$  and  $y = \pi r_c$  [4]. Here,  $y$  represents the extra dimensional coordinate and  $r_c$  is the compactification radius of the extra dimension. The brane which is located at  $y = \pi r_c$  is called the TeV-brane where SM fields live on. The brane at  $y = 0$  is called the Planck-brane. As in the case of ADD model, gravity can propagate to everywhere. TeV and Planck branes have different vacuum energies and the 5 dimensional bulk bounded by these branes has a cosmological constant  $\Lambda$ . Assuming four dimensional Poincare invariance, the solution to Einstein's field equations is given by the following metric [4]:

$$ds^2 = e^{-2k|y|} \eta_{\mu\nu} dx^\mu dx^\nu - dy^2, \quad (10)$$

where  $k$  is a constant of order the Planck scale. It is also deduced from the solution of Einstein's field equations that TeV and Planck branes have equal magnitude but opposite



sign tensions and  $\Lambda < 0$ . Therefore, the spacetime in between TeV and Planck branes is a slice of an  $AdS_5$  geometry. Inserting metric (10) into the action for the gravity and integrating over extra dimensional coordinate  $y$ , we obtain the following relation between the Planck scale and the fundamental scale:

$$\bar{M}_{Pl}^2 = \frac{M^3}{k}(1 - e^{-2kr_c\pi}). \quad (11)$$

If  $k \sim \bar{M}_{Pl}$  and  $e^{-2kr_c\pi}$  is very small then the hierarchy between  $\bar{M}_{Pl}$  and  $M$  is eliminated. From the action for matter fields we can deduce that any mass scale  $m_0$  on the TeV brane in the higher dimensional theory will correspond to a physical mass  $e^{-kr_c\pi}m_0$ . The factor  $e^{-kr_c\pi}$  is called warp factor. If  $kr_c \sim 12$  then the warp factor is small enough to generate TeV scale masses from the masses of order  $M_{Pl}$ . Hence, RS model solves the hierarchy problem without generating a large hierarchy between  $k$  and  $\frac{1}{r_c}$ .

In the RS model, KK graviton mass spacing is quite large compared with the ADD model. The mass spectrum is given by  $m_n = x_n k e^{-kr_c\pi} = x_n \beta \Lambda_\pi$  where  $\beta = k/\bar{M}_{Pl}$  and  $x_n$  are the roots of  $J_1(x_n) = 0$  [50]. Therefore the mass spacing is at the order of TeV scale. Summation in the graviton propagator cannot be approximated to an integral. Instead, discrete graviton mass spectrum should be considered in the summation. Since the contribution of the KK graviton excitations to the propagator is small for masses above the center-of-mass energy of the process, we can cut off the series at some finite mass value. During calculations, we have considered first four roots of the Bessel function. Another important feature of the RS model is that massive KK graviton excitations couple to SM fields with a coupling constant  $\frac{1}{\Lambda_\pi}$  where  $\Lambda_\pi$  is a scale of the order of TeV.

Amplitude square for the process  $\gamma q \rightarrow \gamma q$  in the RS model can be easily obtained from (4) and (5) through the replacement [50]:

$$\frac{1}{\bar{M}_{Pl}^2} D(\hat{t}) \longrightarrow \frac{1}{2\Lambda_\pi^2} \sum_n \frac{1}{\hat{t} - m_n^2 + im_n \Gamma_n} \quad (12)$$

where the decay width for the  $n$ th KK graviton excitation is  $\Gamma_n = \rho m_n (\frac{m_n}{\Lambda_\pi})^2$ . Here,  $\rho$  is a constant which is assumed to be 1.

We have obtained 95% C.L. excluded regions in the  $\beta - m_G$  plane using a similar statistical analysis that was performed for the ADD model. Here,  $m_G$  is the mass of the first KK graviton excitation, i.e.,  $m_G = m_1$ . We present our results in Fig.5 for two different forward detector acceptances  $0.1 < \xi < 0.15$  and  $0.1 < \xi < 0.5$ . The limits for the whole AFP

and CMS-TOTEM acceptance regions are weaker than the limits for  $0.1 < \xi < 0.15$  and  $0.1 < \xi < 0.5$  subintervals. Hence, we do not present them. In the ADD model we have examined the validity of Bjorken scaling by considering three different virtuality values. We have showed that although the Bjorken scaling is not strictly valid, the limits vary a little with  $Q^2$ . We expect the same behavior in the RS model case since we have used the same distribution functions. Therefore, we present our limits only for  $(5M_Z)^2$ .

#### IV. CONCLUSIONS

The potential of  $\gamma\gamma$  processes at the LHC to probe large and warped extra dimensions was investigated in Refs. [27, 32, 39] by some of the authors of this work. In these earlier papers the processes  $pp \rightarrow p\gamma\gamma p \rightarrow p\ell^+\ell^-p$  [27],  $pp \rightarrow p\gamma\gamma p \rightarrow p\gamma\gamma p$  [32] and  $pp \rightarrow p\gamma\gamma p \rightarrow p t\bar{t}p$  [39] were considered and the bounds on model parameters of ADD and RS models were obtained. In our present paper we have probed the large and warped extra dimensions via  $\gamma q \rightarrow \gamma q$  subprocess in a *quasireal photon-proton* deep inelastic scattering at the LHC. In the case of ADD model, the bounds that we have obtained for the  $\gamma q \rightarrow \gamma q$  subprocess are better than the bounds obtained in our earlier papers. For instance, in the acceptance region of  $0.1 < \xi < 0.5$  and  $L_{int} = 100fb^{-1}$  the lower bounds on the cutoff scale  $\Lambda_T$  for the subprocesses  $\gamma\gamma \rightarrow \ell^+\ell^-$ ,  $\gamma\gamma \rightarrow \gamma\gamma$  and  $\gamma\gamma \rightarrow t\bar{t}$  are 3500 GeV, 5100 GeV and 2700 GeV respectively. On the other hand, same bound for  $\gamma q \rightarrow \gamma q$  subprocess exceeds 6000 GeV. In the case of RS model, excluded region of the model parameters extends to wider regions than the case of the subprocesses  $\gamma\gamma \rightarrow \ell^+\ell^-$  and  $\gamma\gamma \rightarrow t\bar{t}$ . When we compare our present bounds with the bounds obtained from the subprocess  $\gamma\gamma \rightarrow \gamma\gamma$ , we see that our present bounds are little better than the bounds from  $\gamma\gamma \rightarrow \gamma\gamma$ . But the difference in bounds is minor especially for low  $\beta$  values. For instance, 95% C.L. lower bounds on the mass of the KK graviton obtained from the subprocess  $\gamma\gamma \rightarrow \gamma\gamma$  are 910 GeV and 1350 GeV for  $\beta = 0.05$  and  $\beta = 0.1$  respectively. Here, the forward detector acceptance is taken to be  $0.1 < \xi < 0.5$  and  $L_{int} = 200fb^{-1}$ . The same bounds for  $\gamma q \rightarrow \gamma q$  subprocess are 965 GeV and 1466 GeV for  $\beta = 0.05$  and  $\beta = 0.1$  respectively. Hence, we can say that the bounds obtained from the subprocess  $\gamma q \rightarrow \gamma q$  are comparable to those obtained from  $\gamma\gamma \rightarrow \gamma\gamma$ .

The reason why the subprocess  $\gamma q \rightarrow \gamma q$  provides more stringent bounds than the above  $\gamma\gamma$  processes, is a consequence of a fact related to quark and photon distributions. In

general, quark distribution functions are bigger in magnitude than equivalent photon distribution functions, i.e., in a proton the probability to find a quark with a Bjorken parameter  $x$  is higher than the probability of a quasireal photon with same momentum fraction  $x$ . Therefore,  $\gamma$ -quark processes have higher effective luminosity than  $\gamma\gamma$  processes. Furthermore, although both quark and quasireal photon distributions decrease as the  $x$  parameter increases, this behavior is drastic in the quasireal photon case. Thus, quarks in general carry more of the proton's energy than quasireal photons. Hence,  $\gamma$ -quark processes have higher energy reach than  $\gamma\gamma$  processes. Due to above reasons, we expect that  $\gamma$ -quark processes have a higher potential in probing new physics compared with  $\gamma\gamma$  processes.

The subprocess  $\gamma q \rightarrow \gamma q$  in the  $\gamma$ -proton collision seems to have lower potential in probing RS model than ADD model of extra dimensions. The reason for this feature is related to the fact that KK graviton contributions in  $\gamma q \rightarrow \gamma q$  take part only in a t-channel exchange diagram. A detailed explanation can be given as follows: In the ADD model, graviton mass spacing in a KK tower is very narrow. Hence, it is assumed that the mass of the KK states is continuously distributed. It is impossible to see the effect of an individual ADD graviton but their cumulative effect might be observable. On the other hand, in the RS model KK graviton mass spacing is quite large,  $\sim \mathcal{O}(TeV)$ . At the LHC energies we hope to discover the first KK excitation which has a mass of order 1 TeV. Due to this discrete mass structure of RS gravitons resonance effects are important in the RS model but they are absent in the case of ADD model. It is obvious that resonance effects are not observed in u or t-channel exchange diagrams. Instead, they appear in processes including s-channel graviton exchange diagrams. For this reason, our bounds on RS model parameters are only slightly better than the bounds from  $\gamma\gamma \rightarrow \gamma\gamma$  although  $\gamma$ -quark processes have higher energy reach and effective luminosity with respect to  $\gamma\gamma$  processes.

Recent results on large and warped extra dimensions from CMS and ATLAS experiments provide stringent limits [51–56]. In the case of ADD model, our limits on  $\Lambda_T$  for an acceptance of  $0.1 < \xi < 0.5$  are better than these current experimental bounds. However, our limits on RS model parameters are weaker than the recent experimental bounds [56]. Therefore the reaction  $pp \rightarrow p\gamma p \rightarrow p\gamma qX$  has a considerable potential in probing large extra dimensions of the ADD model. On the other hand, its potential is relatively low for the case of RS model.

## Acknowledgments

This work has been supported by the Scientific and Technological Research Council of Turkey (TÜBİTAK) in the framework of the project no: 112T085.

## Appendix: Equivalent photon approximation and photon spectrum

Incoming photon beam in the subprocess  $\gamma q \rightarrow \gamma q$  is described by EPA. According to EPA, equivalent photon distribution for photons which are emitted from a proton beam is given through the formula [8–10]:

$$\frac{dN_\gamma}{dE_\gamma dQ^2} = \frac{\alpha}{\pi} \frac{1}{E_\gamma Q^2} \left[ \left(1 - \frac{E_\gamma}{E}\right) \left(1 - \frac{Q_{min}^2}{Q^2}\right) F_E + \frac{E_\gamma^2}{2E^2} F_M \right] \quad (\text{A.1})$$

where

$$Q_{min}^2 = \frac{m_p^2 E_\gamma^2}{E(E - E_\gamma)}, \quad F_E = \frac{4m_p^2 G_E^2 + Q^2 G_M^2}{4m_p^2 + Q^2} \quad (\text{A.2})$$

$$G_E^2 = \frac{G_M^2}{\mu_p^2} = \left(1 + \frac{Q^2}{Q_0^2}\right)^{-4}, \quad F_M = G_M^2, \quad Q_0^2 = 0.71 \text{ GeV}^2 \quad (\text{A.3})$$

In the above formula,  $Q^2$  and  $E_\gamma$  are the virtuality and energy of the photon spectrum.  $E$  is the energy of the incoming proton beam.  $m_p$  and  $\mu_p$  denote the mass and the magnetic moment of the proton.  $F_E$  and  $F_M$  are functions of the electric and magnetic form factors. After integration over  $dQ^2$  in the interval  $Q_{min}^2 - Q_{max}^2$ , equivalent photon distribution can be written as [14]

$$\frac{dN_\gamma}{dE_\gamma} = \frac{\alpha}{\pi E_\gamma} \left(1 - \frac{E_\gamma}{E}\right) \left[ \varphi\left(\frac{Q_{max}^2}{Q_0^2}\right) - \varphi\left(\frac{Q_{min}^2}{Q_0^2}\right) \right]. \quad (\text{A.4})$$

Here, the function  $\varphi$  is defined by

$$\begin{aligned} \varphi(x) = (1 + ay) & \left[ -\ln\left(1 + \frac{1}{x}\right) + \sum_{k=1}^3 \frac{1}{k(1+x)^k} \right] + \frac{y(1-b)}{4x(1+x)^3} \\ & + c \left(1 + \frac{y}{4}\right) \left[ \ln\left(\frac{1-b+x}{1+x}\right) + \sum_{k=1}^3 \frac{b^k}{k(1+x)^k} \right] \end{aligned} \quad (\text{A.5})$$

where

$$\begin{aligned} y &= \frac{E_\gamma^2}{E(E - E_\gamma)}, \quad a = \frac{1 + \mu_p^2}{4} + \frac{4m_p^2}{Q_0^2} \approx 7.16 \\ b &= 1 - \frac{4m_p^2}{Q_0^2} \approx -3.96, \quad c = \frac{\mu_p^2 - 1}{b^4} \approx 0.028 \end{aligned} \quad (\text{A.6})$$

The contribution to the integral above  $Q_{max}^2 \approx 2 \text{ GeV}^2$  is negligible. Therefore during calculations we set  $Q_{max}^2 = 2 \text{ GeV}^2$ .

---

- [1] N. Arkani-Hamed, S. Dimopoulos and G. R. Dvali, Phys. Lett. B **429**, 263 (1998) [hep-ph/9803315].
- [2] N. Arkani-Hamed, S. Dimopoulos and G. R. Dvali, Phys. Rev. D **59**, 086004 (1999) [hep-ph/9807344].
- [3] I. Antoniadis, N. Arkani-Hamed, S. Dimopoulos and G. R. Dvali, Phys. Lett. B **436**, 257 (1998) [hep-ph/9804398].
- [4] L. Randall and R. Sundrum, Phys. Rev. Lett. **83**, 3370 (1999) [hep-ph/9905221].
- [5] X. Rouby, Ph.D. thesis, Universite Catholique de Louvain [UCL-Thesis 135-2008 and CMS TS-2009/004, 2008].
- [6] J. de Favereau de Jeneret, V. Lemaitre, Y. Liu, S. Oryn, T. Pierzchala, K. Piotrkowski, X. Rouby, N. Schul and M. Vander Donckt, arXiv:0908.2020 [hep-ph].
- [7] N. Schul, Ph.D. thesis, Universite Catholique de Louvain [CERN-THESIS-2011-271 and CMS-TS-2011-030].
- [8] V. M. Budnev, I. F. Ginzburg, G. V. Meledin and V. G. Serbo, Phys. Rep. **15**, 181 (1975).
- [9] G. Baur *et al.*, Phys. Rep. **364**, 359 (2002).
- [10] K. Piotrkowski, Phys. Rev. D **63**, 071502 (2001) [hep-ex/0009065].
- [11] C. Royon *et al.* (RP220 Collaboration), arXiv:0706.1796 [physics.ins-det], *Proceedings for the DIS 2007 workshop, Munich, 2007*.
- [12] M.G. Albrow *et al.* (FP420 R and D Collaboration), J. Instrum. **4**, T10001 (2009); arXiv:0806.0302 [hep-ex].
- [13] V. Avati and K. Osterberg, Report No. CERN-TOTEM-NOTE-2005-002, 2006.
- [14] O. Kepka and C. Royon, Phys. Rev. D **78**, 073005 (2008); arXiv:0808.0322 [hep-ph].
- [15] A. Abulencia *et al.* (CDF Collaboration), Phys. Rev. Lett. **98**, 112001 (2007); arXiv:hep-ex/0611040.
- [16] T. Aaltonen *et al.* (CDF Collaboration), Phys. Rev. Lett. **102**, 222002 (2009); arXiv:0902.2816 [hep-ex].
- [17] T. Aaltonen *et al.* (CDF Collaboration), Phys. Rev. Lett. **102**, 242001 (2009); arXiv:0902.1271

- [hep-ex].
- [18] S. Chatrchyan *et al.* [CMS Collaboration], JHEP **1201**, 052 (2012) [arXiv:1111.5536 [hep-ex]].
  - [19] S. Chatrchyan *et al.* [CMS Collaboration], JHEP **1211**, 080 (2012) [arXiv:1209.1666 [hep-ex]].
  - [20] I. F. Ginzburg and A. Schiller, Phys. Rev. D **57**, 6599 (1998) [hep-ph/9802310].
  - [21] I. F. Ginzburg and A. Schiller, Phys. Rev. D **60**, 075016 (1999) [hep-ph/9903314].
  - [22] V.A. Khoze, A.D. Martin and M.G. Ryskin, Eur. Phys. J. C **23**, 311 (2002); arXiv:hep-ph/0111078.
  - [23] N. Schul and K. Piotrkowski, Nucl. Phys. B, Proc. Suppl., **179**, 289 (2008); arXiv:0806.1097 [hep-ph].
  - [24] S. M. Lietti, A. A. Natale, C. G. Roldao and R. Rosenfeld, Phys. Lett. B **497**, 243 (2001); arXiv:hep-ph/0009289.
  - [25] T. Pierzchala and K. Piotrkowski, Nucl. Phys. Proc. Suppl. **179-180**, 257 (2008); arXiv:0807.1121 [hep-ph].
  - [26] E. Chapon, C. Royon and O. Kepka, Phys. Rev. D **81**, 074003 (2010); arXiv:0912.5161 [hep-ph].
  - [27] S. Atağ, S. C. İnan and İ. Şahin, Phys. Rev. D **80**, 075009 (2009); arXiv:0904.2687 [hep-ph].
  - [28] İ. Şahin and S. C. İnan, JHEP **09**, 069 (2009); arXiv:0907.3290 [hep-ph].
  - [29] T. Dougall and S. D. Wick, Eur. Phys. J. A **39**, 213 (2009) [arXiv:0706.1042 [hep-ph]].
  - [30] M. Chaichian, P. Hoyer, K. Huitu, V. A. Khoze and A. D. Pilkington, JHEP **0905**, 011 (2009) [arXiv:0901.3746 [hep-ph]].
  - [31] K. Piotrkowski and N. Schul, AIP Conf. Proc. **1200**, 434 (2010) [arXiv:0910.0202 [hep-ph]].
  - [32] S. Atağ, S. C. İnan and İ. Şahin, JHEP **09**, 042 (2010); arXiv:1005.4792 [hep-ph].
  - [33] V. P. Goncalves and W. K. Sauter, Phys. Rev. D **82**, 056009 (2010) [arXiv:1007.5487 [hep-ph]].
  - [34] S. C. İnan, Phys. Rev. D **81**, 115002 (2010); arXiv:1005.3432 [hep-ph].
  - [35] S. Atağ and A. A. Billur, JHEP **11**, 060 (2010); arXiv:1005.2841 [hep-ph].
  - [36] M.G. Albrow, T.D. Coughlin and J.R. Forshaw, Prog. Part. Nucl. Phys. **65**, 149-184 (2010); arXiv:1006.1289 [hep-ph].
  - [37] İ. Şahin, and A. A. Billur, Phys. Rev. D **83**, 035011 (2011); arXiv:1101.4998 [hep-ph].
  - [38] İ. Şahin, and M. Koksall, JHEP **03**, 100 (2011); arXiv:1010.3434 [hep-ph].
  - [39] S. C. Inan and A. A. Billur, Phys. Rev. D **84**, 095002 (2011).
  - [40] R. S. Gupta, Phys. Rev. D **85**, 014006 (2012) [arXiv:1111.3354 [hep-ph]].

- [41] İ. Şahin, Phys. Rev. D **85**, 033002 (2012) [arXiv:1201.4364 [hep-ph]].
- [42] L. N. Epele, H. Fanchiotti, C. A. G. Canal, V. A. Mitsou and V. Vento, Eur. Phys. J. Plus **127**, 60 (2012) [arXiv:1205.6120 [hep-ph]].
- [43] B. Şahin and A. A. Billur, Phys. Rev. D **86**, 074026 (2012) [arXiv:1210.3235 [hep-ph]].
- [44] İ. Şahin and B. Şahin, Phys. Rev. D **86**, 115001 (2012) [arXiv:1211.3100 [hep-ph]].
- [45] A. A. Billur, Europhys. Lett. **101**, 21001 (2013).
- [46] A. Senol, Phys. Rev. D **87**, 073003 (2013) [arXiv:1301.6914 [hep-ph]].
- [47] G. F. Giudice, R. Rattazzi and J. D. Wells, Nucl. Phys. B **544**, 3 (1999) [hep-ph/9811291].
- [48] T. Han, J. D. Lykken and R. -J. Zhang, Phys. Rev. D **59**, 105006 (1999) [hep-ph/9811350].
- [49] A. D. Martin, W. J. Stirling, R. S. Thorne and G. Watt, Eur. Phys. J. C **63**, 189 (2009) [arXiv:0901.0002 [hep-ph]].
- [50] H. Davoudiasl, J. L. Hewett and T. G. Rizzo, Phys. Rev. Lett. **84**, 2080 (2000) [hep-ph/9909255].
- [51] M. Marionneau [on behalf of the ATLAS and CMS Collaboration], arXiv:1305.3169 [hep-ex].
- [52] ATLAS Collaboration, ATLAS-CONF-2012-147.
- [53] CMS Collaboration, CMS-PAS-EXO-12-027.
- [54] CMS Collaboration, CMS-PAS-EXO-12-031.
- [55] G. Aad *et al.* [ATLAS Collaboration], Phys. Rev. D **87**, 015010 (2013) [arXiv:1211.1150 [hep-ex]].
- [56] G. Aad *et al.* [ATLAS Collaboration], New J. Phys. **15**, 043007 (2013) [arXiv:1210.8389 [hep-ex]].

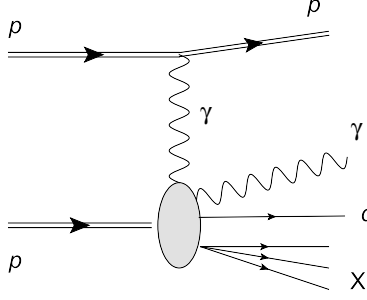


FIG. 1: Schematic diagram for the reaction  $pp \rightarrow p\gamma p \rightarrow p\gamma q X$ .

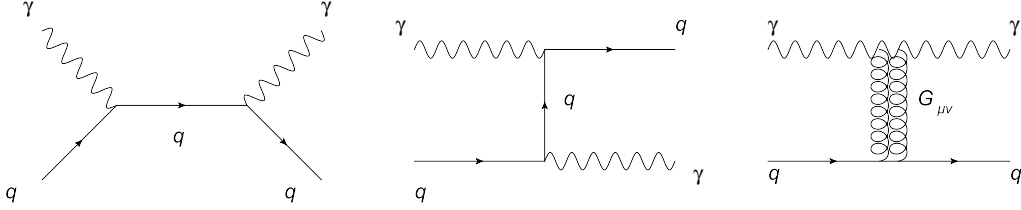


FIG. 2: Tree-level Feynman diagrams for the subprocess  $\gamma q \rightarrow \gamma q$  ( $q = u, d, c, s, b, \bar{u}, \bar{d}, \bar{c}, \bar{s}, \bar{b}$ ) in the presence of Kaluza-Klein graviton mediation.

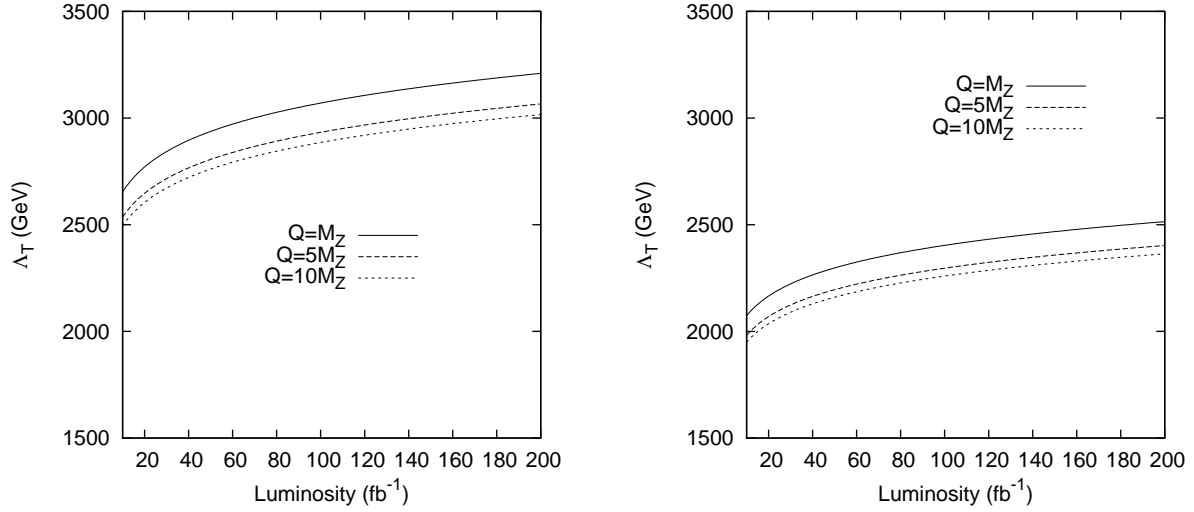


FIG. 3: 95% C.L. lower bounds for  $\Lambda_T$  as a function of integrated LHC luminosity for forward detector acceptance regions  $0.0015 < \xi < 0.5$  (left panel) and  $0.0015 < \xi < 0.15$  (right panel). Legends are for various values of the virtuality of the deep inelastic scattering.



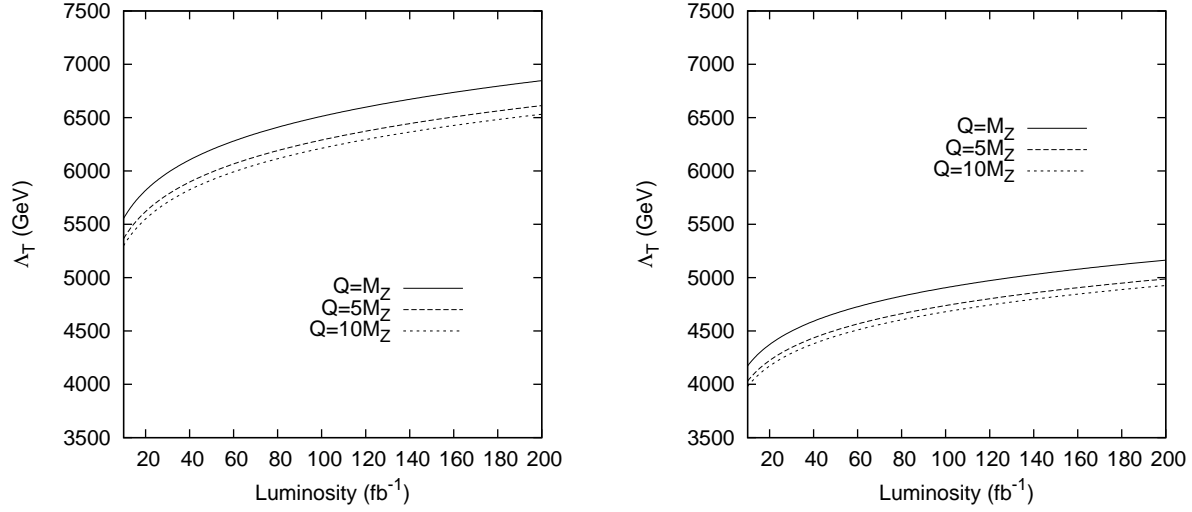


FIG. 4: 95% C.L. lower bounds for  $\Lambda_T$  as a function of integrated LHC luminosity for forward detector acceptance regions  $0.1 < \xi < 0.5$  (left panel) and  $0.1 < \xi < 0.15$  (right panel). Legends are for various values of the virtuality of the deep inelastic scattering.

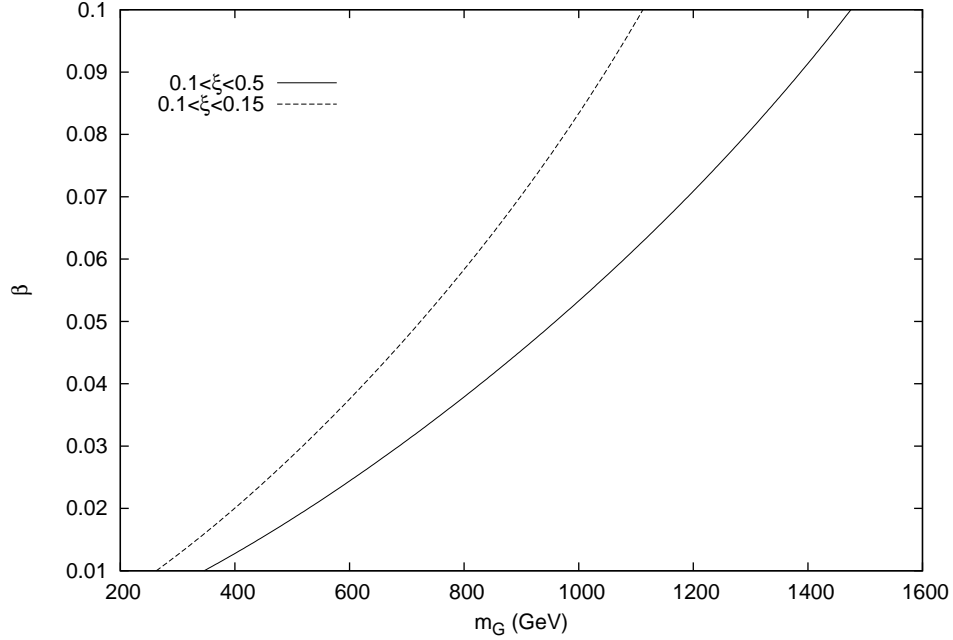


FIG. 5: Limits in the  $\beta - m_G$  plane for an integrated luminosity of  $200 fb^{-1}$ . The regions above the curves are excluded at 95% C.L. The virtuality of the deep inelastic scattering is taken to be  $Q^2 = (5M_Z)^2$  where  $M_Z$  is the mass of the Z boson.